THE JOURNAL OF BIOLOGICAL CHEMISTRY
Vol. 278, No. 31, Issue of August 1, pp. 28993–28999, 2003

Printed in U.S.A.

Contrasting Membrane Interaction Mechanisms of AP180 N-terminal Homology (ANTH) and Epsin N-terminal Homology (ENTH) Domains*

Received for publication, March 20, 2003, and in revised form, May 8, 2003
Published, JBC Papers in Press, May 8, 2003, DOI 10.1074/jbc.M302865200

Robert V. Stahelin‡, Fei Long‡, Brian J. Peter§¶, Diana Murray‖, Pietro De Camilli, Harvey T. McMahon§, and Wonhwa Cho‡ ‡‡**

*From the ‡Department of Chemistry, University of Illinois at Chicago, Chicago, Illinois 60607, the §Medical Research Council Laboratory of Molecular Biology, Hills Road, Cambridge CB2 2QH, United Kingdom, the ‖Department of Microbiology and Immunology, Weill Medical College of Cornell University, New York, New York 10021, and the **Howard Hughes Medical Institute and Department of Cell Biology, Yale University School of Medicine, New Haven, Connecticut 06510*

Epsin and AP180/CALM are endocytotic accessory proteins that have been implicated in the formation of clathrin-coated pits. Both proteins have phosphatidylinositol 4,5-bisphosphate (PtdIns(4,5)P_2)-binding domains in their N termini, but these domains are structurally and functionally different. To understand the basis of their distinct properties, we measured the PtdIns(4,5)P_2-dependent membrane binding of the epsin N-terminal homology (ENTH) domain and the AP180 N-terminal homology (ANTH) domain by means of surface plasmon resonance and monolayer penetration techniques and also calculated the effect of PtdIns(4,5)P_2 on the electrostatic potential of these domains. PtdIns(4,5)P_2 enhances the electrostatic membrane association of both domains; however, PtdIns(4,5)P_2 binding exerts distinct effects on their membrane dissociation. Specifically, PtdIns(4,5)P_2 induces the membrane penetration of the N-terminal α-helix of the ENTH domain, which slows the membrane dissociation of the domain and triggers the membrane deformation. These results provide the biophysical explanation for the membrane bending activity of epsin and its ENTH domain.

Clathrin-mediated endocytosis is an energetically demanding process that is necessary for a diverse number of cellular processes, such as nutrient uptake, removal of receptors from the cell surface, and synaptic vesicle recycling (1–3). This process involves cooperation of clathrin, the AP-2 adaptor complex and a number of other accessory proteins, including epsin. The process of endocytosis occurs through four general steps including bud initiation, bud formation, bud constriction, and vesicle scission (2, 3). Initiation of the bud site is thought to occur by the membrane association of AP180 and epsin as well as the adaptor complex AP-2. These proteins recruit clathrin to the membrane. The bud then forms and constricts, while the activities of amphiphysin and endophilin remodel the membrane at the bud neck. Finally, the GTPase activity of dynamin is required for the release of the vesicle into the cytoplasm (4). Recently, the importance of phosphatidylinositol 4,5-bisphosphate (PtdIns(4,5)P_2)[1] in clathrin-mediated endocytosis has come to light (5). In particular, epsin and AP180, which are necessary for the formation of clathrin-coated vesicles, bind PtdIns(4,5)P_2 through their conserved N-terminal domains (6–8).

The epsin N-terminal homology (ENTH) domain (9–13) is a highly conserved domain of ~140 amino acids that has been identified in all epsins and binds PtdIns(4,5)P_2 with high affinity and specificity (6–8). The ENTH domain is made of a superhelix of 7 α-helices with an eighth α-helix misaligned with the superhelical axis, which is structurally similar to the superhelical VHS domain (14). The AP180/CALM and HIP1/HIP1R protein families contain an N-terminal domain that is homologous to the ENTH domain and binds PtdIns(4,5)P_2 (13). X-ray structural analysis of the AP180 N-terminal homology (ANTH) domains of AP180/CALM (7) showed that the ANTH domain is extended by one or more α-helices when compared with the ENTH domain.

Both the AP180 ANTH domain and the epsin ENTH domain bind PtdIns(4,5)P_2 with high specificity, but structurally in a different manner. The ANTH domain binds PtdIns(4,5)P_2 via solvent-exposed Lys and His side chains on one side of the domain, and only the lipid headgroup is contacted by the protein (7). The ENTH domain binds PtdIns(4,5)P_2 in a pocket and makes extensive contacts with both the headgroup and glycerol backbone (8). On binding the PtdIns(4,5)P_2 headgroup, residues 3–15 of the ENTH domain adopt an α-helical structure which makes up one side of the PtdIns(4,5)P_2-binding pocket and provides ionic interactions. The outer surface of this amphipathic helix, termed helix 0, was proposed to lie in the plane of the lipid bilayer with the Leu^6, Met^{10}, and Ile^{13} residues buried into the hydrophobic phase. This insertion of helix 0 was proposed to displace the lipid headgroups thus driving membrane curvature (8). A number of mutations of the hydrophobic

* This work was supported by National Institutes of Health Grants GM66147 (to D. M.) and GM52598 and GM53987 (to W. C.). The costs of publication of this article were defrayed in part by the payment of page charges. This article must therefore be hereby marked "*advertisement*" in accordance with 18 U.S.C. Section 1734 solely to indicate this fact.

¶ Supported by an European Molecular Biology Long Term Postdoctoral Fellowship.

‡‡ To whom correspondence should be addressed: Dept. of Chemistry (M/C 111), University of Illinois at Chicago, 845 West Taylor St., Chicago, IL 60607-7061. Tel.: 312-996-4883; Fax: 312-996-2183; E-mail: wcho@uic.edu.

[1] The abbreviations used are: PtdIns(4,5)P_2, phosphatidylinositol 4,5-bisphosphate; ANTH, AP180 N-terminal homology; ENTH, epsin N-terminal homology; Ins(1,4,5)P_3, inositol 1,4,5-triphosphate; POPC, 1-palmitoyl-2-oleoyl-*sn*-glycero-3-phosphocholine; POPE, 1-palmitoyl-2-oleoyl-*sn*-glycero-3-phosphoehthanolamine; POPS, 1-palmitoyl2-oleoyl-*sn*-glycero-3-phosphoserine; SPR, surface plasmon resonance; CHAPS, 3-[3-cholamidopropyl)dimethylammonio]-1-propanesulfonic acid.

residues were used to advance this hypothesis; however, biophysical evidence for membrane insertion of the epsin ENTH domain has not been shown.

In this study, we investigated the effect of PtdIns(4,5)P_2 on the membrane binding of the epsin ENTH and the AP180 ANTH domains by surface plasmon resonance (SPR) and monolayer analyses. Results from these measurements as well as the calculation of their electrostatic potential in the absence and presence of PtdIns(4,5)P_2 indicate that the ENTH and ANTH domains have distinctly different modes of membrane interaction.

EXPERIMENTAL PROCEDURES

Materials—1-Palmitoyl-2-oleoyl-*sn*-glycero-3-phosphocholine (POPC), 1-palmitoyl-2-oleoyl-*sn*-glycero-phosphoethanolamine (POPE), and 1-palmitoyl-2-oleoyl-*sn*-glycero-3-phosphoserine (POPS) were from Avanti Polar Lipids (Alabaster, AL). 1,2-Dipalmitoyl derivatives of phosphatidylinositol 3,5-bisphosphate, phosphatidylinositol 3,4,5-triphosphate, and PtdIns(4,5)P_2 were a kind gift from Dr. Karol Bruzik. Phospholipid concentrations were determined by phosphate analysis (15). Restriction endonucleases and other enzymes for molecular biology were from New England Biolabs (Beverly, MA). CHAPS and octyl glucoside were from Sigma and Fisher Scientific, respectively. The liposofast microextruder and 100-nm polycarbonate filters were from Avestin (Ottawa, Ontario). Pioneer L1 sensor chip was from Biacore AB (Piscataway, NJ).

Mutagenesis and Protein Expression—The R114A mutant of epsin ENTH was prepared by the overlap extension polymerase chain reaction method (16), and all other mutants were prepared as described previously (8). Each construct was subcloned into the pGEX-4T-1 vector containing a N-terminal glutathione *S*-transferase fusion and transformed into *Escherichia coli* DH5α cells for plasmid isolation. After verifying the DNA sequence, the plasmid was transformed into *E. coli* BL21 cells for protein expression. One liter of 2× YT medium (16 g of tryptone, 10 g of yeast extract, and 5 g of NaCl in 1 liter of H_2O) containing 100 μg/ml ampicillin was inoculated with BL21 cells harboring each construct and grown at 37 °C until absorbance at 600 nm reached 0.4. At this time, 20 mg of isopropyl-1-thio-β-D-galactopyranoside was added, and cells were then incubated at 25 °C for 16 h.

Cells were harvested for 10 min at 4,000 × *g*, and the resulting pellet was resuspended in 10 ml of 20 mM Tris-HCl, pH 8.0, containing 0.16 M NaCl, 50 μM phenylmethylsulfonyl fluoride, and 0.1% Triton X-100. The solution was then sonicated for 8 min using a 30-s sonication followed by 30-s cooling on ice. This was followed by centrifugation at 48,000 × *g* to separate the soluble and insoluble fractions. The supernatant was filtered into a 50-ml tube, and 1 ml of GST·Tag™ resin (Novagen, Madison, WI) was added. The mixture was incubated on ice with gentle stirring (80 rpm) for 30 min. After this time, the mixture was poured onto a column, which was washed with 20 ml of 20 mM Tris-HCl, pH 8.0, containing 0.16 M NaCl. The column was then sealed and 1 ml of 20 mM Tris-HCl, pH 8.0, containing 0.16 M NaCl and 0.25 mM $CaCl_2$ along with 2 units of thrombin were added to cleave the glutathione *S*-transferase tag. After 6 h at 25 °C, the protein was eluted from the column in 5 fractions using 1 ml of 20 mM Tris, pH 8.0, containing 0.16 M NaCl. Purity was checked on an 18% polyacrylamide gel, and samples were pooled and concentrated to 1 ml. Protein concentration was then determined using the BCA method (Pierce). The AP180 ANTH domain was purified as described previously (8).

Monolayer Penetration Experiments—The penetration of ENTH and ANTH domains into the phospholipid monolayer was measured at 23 °C by monitoring the change in surface pressure (π) at constant surface area using a circular Teflon trough (4-cm diameter and 1-cm depth) and Wilhelmy plate connected to a Cahn microbalance as described previously (17). A lipid monolayer containing various combinations of phospholipids was spread onto the subphase composed of 10 mM HEPES, pH 7.4, containing 0.16 M NaCl until the desired initial surface pressure (π_0) was reached. After the signal stabilized (~5 min), 50 μg of proteins were injected to the subphase through the hole in the wall of the trough, and the change in surface pressure ($\Delta\pi$) was monitored for 45 min while stirring the subphase at 60 rpm. Typically, the $\Delta\pi$ value reached a maximum after 20 min. It has been shown empirically that $\Delta\pi$ caused by protein is mainly due to the penetration of the protein into the lipid monolayer. For example, in the case of the C2 domain of group IVA cytosolic phospholipase A_2, excellent agreement was found between large $\Delta\pi$ caused by several residues in the calcium-binding loops (17) and their actual membrane penetration measured by fluorescence (18) and electron spin resonance studies (19, 20). The maximal $\Delta\pi$ value depended on the protein concentration and reached a saturation value (*e.g.* [epsin ENTH] ≥ 3.0 μg/ml); therefore, protein concentration in the subphase was maintained above such values to ensure that the observed $\Delta\pi$ represented a maximum value. The resulting $\Delta\pi$ was plotted *versus* π_0 from which the critical surface pressure (π_c) was determined as the *x* intercept (21, 22).

Kinetic and Equilibrium SPR Experiments—All SPR binding measurements were performed at 23 °C. The coating of the L1 sensor chip has been described in detail previously (23, 24). The sensor chip surface was washed and then coated by injecting 90 μl of vesicles containing various phospholipids (see "Results") at 5 μl/min to give a response of 6,000 resonance units. Similarly, a control surface was coated with vesicles, typically without phosphoinositide of interest, to give the same resonance unit response as the active binding surface. Under our experimental conditions, no binding was detected to this control surface beyond the refractive index change for the ENTH and ANTH domains. Each lipid layer was stabilized by injecting 10 μl of 50 mM NaOH three times at 100 μl/min. Typically, no decrease in lipid signal was seen after the first injection. Kinetic SPR measurements were done at the flow rate of 30 μl/min. 30 μl of protein in 10 mM HEPES, pH 7.4, containing 0.16 M KCl was injected to give an association time of 60 s, while the dissociation was monitored for 400 s at which time the protein had completely dissociated. The lipid surface was washed with 10 μl of 50 mM NaOH before the next protein injection.

After sensorgrams were obtained for five different concentrations of each protein within a 10-fold range of K_d, each of the sensorgrams was corrected for refractive index change by subtracting the control surface response from it. The association and dissociation phases of all sensorgrams were globally fit to a 1:1 Langmuir binding model: protein + (protein-binding site on the vesicle) ↔ (complex) using BIAevalutation 3.0 software (Biacore) as described previously (24–26). The dissociation constant (K_d) was then calculated from the equation, $K_d = k_d/k_a$. Mass transport (27, 28) was not a limiting factor in our experiments, as change in flow rate (5 μl/min to 60 μl/min) did not affect kinetics of association and dissociation. After curve fitting, residual plots and χ^2 values were checked to verify the validity of the binding model. Each data set was repeated three times to calculate a standard deviation. Also, K_d values were separately determined from equilibrium SPR measurements. For these measurements, the flow rate was reduced to 2 μl/min to allow sufficient time for the association phase, which in turn allows resonance unit values to reach saturating response values (R_{eq}). R_{eq} values were then plotted *versus* protein concentrations (*C*), and the K_d value was determined by a non-linear least squares analysis of the binding isotherm using an equation, $R_{eq} = R_{max}/(1 + K_d/C)$, where R_{max} is a maximal R_{eq} value. K_d values obtained by both kinetic and equilibrium analysis for epsin ENTH and AP180 ANTH were in agreement (data not shown), thus validating the kinetic analysis.

It should be noted that in our SPR analysis K_d is defined in terms of not the molarity of phospholipids but the molarity of protein-binding sites on the vesicle. Thus, if each protein-binding site on the vesicle is composed of *n* lipids, nK_d is the dissociation constant in terms of molarity of lipid monomer (22). Due to difficulty involved in accurate determination of the concentration of lipids coated on the sensor chip, only K_d was determined in our SPR analysis and the relative affinity was calculated as a ratio of K_d values assuming that *n* values are similar for wild type and mutants. This assumption is based on our finding that R_{max} values, which are proportional to [total lipid]/*n* (22), were similar (within 10%) for all proteins under our experimental conditions in which the sensor chip was coated with the same amount of lipids.

Electrostatic Potential Computation—The electrostatic potentials of ENTH and ANTH domains with and without inositol 1,4,5-triphosphate (Ins(1,4,5)P_3) were calculated with a modified version of the program DelPhi and visualized in the program GRASP (29), as described previously (30). In the panels of Fig. 3, the electrostatic potentials are represented by two-dimensional equipotential contours in 0.1 M KCl, with *red* and *blue* indicating negative and positive potentials, respectively. The electrostatic calculations performed used partial charges taken from the CHARMM27 (31) force field and spatial coordinates taken from the structures of free epsin ENTH (1INZ) (32), Ins(1,4,5)P_3-bound epsin ENTH (1H0A) (8), and CALM ANTH (1HFA) (7).

RESULTS

Monolayer Penetration Analysis of ENTH and ANTH Domains—Recent studies have indicated that phosphoinositides can induce the membrane penetration of FYVE (26) and PX

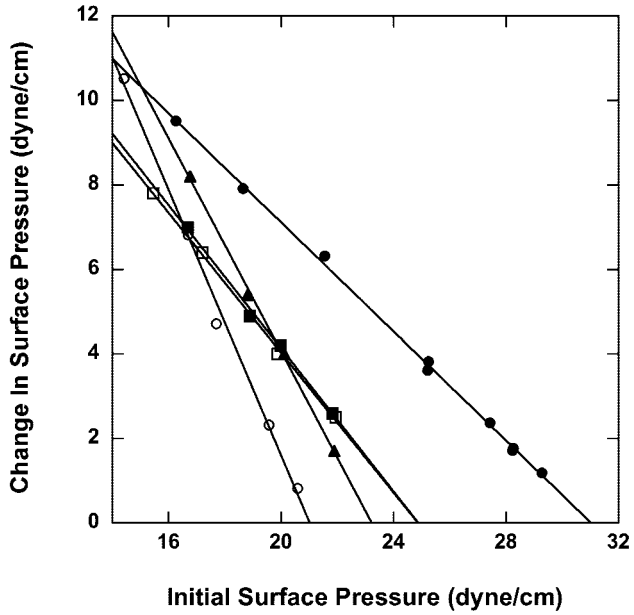

FIG. 1. **Monolayer penetration of epsin ENTH and AP180 ANTH domains.** $\Delta\pi$ was monitored as a function of π_0 values for epsin ENTH (○) and AP180 ANTH (□) with a POPC/POPE (80:20) monolayer. The same measurements were performed for epsin ENTH (●) and AP180 ANTH (■) with a POPC/POPE/PtdIns(4,5)P_2 (77:20:3) monolayer. Also, the penetration of epsin ENTH into a POPC/POPE/phosphatidylinositol 3,4-bisphosphate (77:20:3) monolayer (▲) was measured. The subphase was 10 mM HEPES buffer, pH 7.4, with 0.16 M KCl for all measurements.

domains (33). To see if PtdIns(4,5)P_2 can also elicit the membrane penetration of ENTH and ANTH domains, we measured the interactions of epsin ENTH and AP180 ANTH domains with phospholipid monolayers in the presence and absence of PtdIns(4,5)P_2. Phospholipid monolayers at the air-water interface serve as a highly sensitive tool to measure the membrane penetrating ability of protein (22, 34–36). In these studies, POPC/POPE (80:20) or POPC/POPE/PtdIns(4,5)P_2 (77:20:3) monolayers of a given initial surface pressure (π_0) were spread at constant area and the change in surface pressure ($\Delta\pi$) was monitored after the injection of the protein into the subphase. In general, $\Delta\pi$ is inversely proportional to π_0 of the phospholipid monolayer and an extrapolation of the $\Delta\pi$ versus π_0 plot yields the critical surface pressure (π_c), which specifies an upper limit of π_0 of a monolayer that a protein can penetrate into (21, 22). Since the surface pressure of cell membranes and large unilamellar vesicles has been estimated to be in the range of 30–35 dyne/cm (37–39), for a protein to penetrate these bilayer membranes its π_c value should be above 30 dyne/cm. Fig. 1 shows that toward the POPC/POPE (80:20) monolayer both epsin ENTH and AP180 ANTH domains have low intrinsic penetrating ability with π_c values of 21 and 24 dyne/cm, respectively. However, the addition of 3 mol % PtdIns(4,5)P_2 to the monolayer (*i.e.* POPC/POPE/PtdIns(4,5)P_2 (77:20:3)) increased the π_c value of the epsin ENTH domain to 32 dyne/cm, suggesting that PtdIns(4,5)P_2 might allow penetration of the domain into cell membranes and large unilamellar vesicles. The specific nature of PtdIns(4,5)P_2 activation was evidenced by a much smaller effect of 3 mol % phosphatidylinositol 3,4-bisphosphate (Fig. 1) on the π_c value for the epsin ENTH domain. Furthermore, neither 3 mol % phosphatidylinositol 3,4,5-triphosphate nor 30 mol % POPS had a significant effect (data not shown). Interestingly, the incorporation of 3 mol% PtdIns(4,5)P_2 into the POPC/POPE (80:20) monolayer did not significantly change the π_c value of the AP180 ANTH domain, showing that PtdIns(4,5)P_2 does not induce the membrane penetration of the AP180 ANTH domain. This also suggests that the ANTH domain cannot effectively penetrate compactly packed lipid bilayers, including cell membranes, even in the presence of PtdIns(4,5)P_2.

Surface Plasmon Resonance Measurements of Membrane Binding of ENTH and ANTH Domains—The lipid headgroup specificity of the epsin ENTH domain and the AP180 ANTH domain has been determined using soluble inositol lipids. For instance, the epsin ENTH domain binds monomeric Ins(1,4,5)P_3 (K_d = 3.6 μM) 33 times more strongly than monomeric inositol 1,3,5-triphosphate (8). Also, the epsin ENTH domain has 8-fold higher affinity for Ins(1,4,5)P_3 than the AP180 ANTH domain (8). However, their specificity and affinity for membrane-incorporated phosphoinositides has not been fully investigated. We first measured the affinity of the epsin ENTH domain for various phosphoinositide-containing vesicles (*i.e.* POPC/POPE/phosphoinositide (77:20:3)) using POPC/POPE (80:20) vesicles as a control. As listed in Table I, the epsin ENTH domain showed high affinity for POPC/POPE/PtdIns(4,5)P_2 (77:20:3) vesicles (K_d = 23 ± 7 nM). It should be noted that for our SPR vesicle binding analysis K_d is defined as the dissociation constant for vesicle binding (not for phosphoinositide binding) in terms of the molarity of protein-binding sites on the vesicle, which is composed of n lipids (22) (see "Experimental Procedures"). Thus, the large difference between the K_d for monomeric Ins(1,4,5)P_3 and the K_d for POPC/POPE/PtdIns(4,5)P_2 (77:20:3) vesicles does not reflect the different affinities of the domain for monomeric and membrane-incorporated PtdIns(4,5)P_2. When compared with POPC/POPE/PtdIns(4,5)P_2 (77:20:3) vesicles, the epsin ENTH domain had much lower affinity for POPC/POPE/phosphatidylinositol 3,4-bisphosphate (77:20:3) and POPC/POPE/phosphatidylinositol 3,4,5-trisphosphate (77:20:3) vesicles. Lower estimates of K_d for these vesicles assessed from the protein concentrations employed for the SPR measurements were 10 μM, indicating that the epsin ENTH domain prefers membrane-incorporated PtdIns(4,5)P_2 to other phosphoinositides by more than two orders of magnitude.

The AP180 ANTH domain also had high specificity for PtdIns(4,5)P_2-containing vesicles. For the same POPC/POPE/PtdIns(4,5)P_2 (77:20:3) vesicles; however, the AP180 ANTH domain showed 12-fold lower affinity than the epsin ENTH domain. This difference in K_d is due to a 2.7-fold larger k_a and a 4.3-fold smaller k_d for the ENTH domain. The membrane association of peripheral proteins can be accelerated by long range electrostatic interactions (24), and the larger k_a for the ENTH domain is consistent with its more positive electrostatic potential, especially around the PtdIns(4,5)P_2-binding site when compared with the ANTH domain (6–8) (see also Fig. 3). On the other hand, the membrane dissociation step of peripheral proteins can be slowed by short range specific interactions and membrane penetration of hydrophobic residues (24). Thus, the smaller k_d value of the epsin ENTH domain in comparison to the AP180 ANTH domain is consistent with our monolayer penetration data showing that the former penetrates more effectively into PtdIns(4,5)P_2-containing monolayers than the latter. To further demonstrate that PtdIns(4,5)P_2 has differential effects on the membrane binding of the ENTH and ANTH domains, we measured the vesicle binding of these domains as a function of PtdIns(4,5)P_2 and KCl concentrations. When the PtdIns(4,5)P_2 content in the vesicles was reduced from 3 to 0.5 mol %, the k_a decreased 5.4- and 9-fold for the epsin ENTH domain and the AP180 ANTH domain, respectively. However, the reduction in PtdIns(4,5)P_2 content had little effect on the k_d of the ANTH domain but caused a 2-fold increase the k_d for epsin ENTH. This difference again underscores the specific

TABLE I

Binding parameters for epsin-ENTH, AP180-ANTH, and epsin ENTH mutants determined from SPR analysis

Values represent the mean and S.D. from three determinations. All measurements were performed in 10 mM HEPES, pH 7.4, containing 0.16 M KCl unless specified otherwise.

Proteins	k_a	k_d	k_d	Fold increase in K_d[a]
	$M^{-1}\ s^{-1}$	s^{-1}	M	
POPC/POPE/PtdIns(4,5)P_2 (77:20:3)				
ENTH	$(1.3 \pm 0.3) \times 10^6$	$(3.0 \pm 0.6) \times 10^{-2}$	$(2.3 \pm 0.7) \times 10^{-8}$	1
ENTH L6Q	$(4.3 \pm 0.5) \times 10^5$	$(1.2 \pm 0.4) \times 10^{-1}$	$(2.8 \pm 1.0) \times 10^{-7}$	12
ENTH M10Q	$(2.4 \pm 0.3) \times 10^5$	$(2.1 \pm 0.6) \times 10^{-1}$	$(8.8 \pm 2.7) \times 10^{-7}$	38
ENTH R63L/H73L	NM[b]	NM	NM	
ENTH R114A	$(2.2 \pm 0.5) \times 10^5$	$(2.3 \pm 0.4) \times 10^{-2}$	$(1.0 \pm 0.4) \times 10^{-7}$	4
ANTH	$(4.8 \pm 0.6) \times 10^5$	$(1.3 \pm 0.4) \times 10^{-1}$	$(2.7 \pm 0.9) \times 10^{-7}$	12
POPC/POPE/PtdIns(4,5)P_2 (79.5:20:0.5)				
ENTH	$(2.4 \pm 0.5) \times 10^5$	$(6.1 \pm 0.7) \times 10^{-2}$	$(2.5 \pm 0.6) \times 10^{-7}$	11
ANTH	$(5.3 \pm 0.7) \times 10^4$	$(1.8 \pm 0.5) \times 10^{-1}$	$(3.4 \pm 1.0) \times 10^{-6}$	148
POPC/POPE/PtdIns(4,5)P_2 (77:20:3) with 0.5 M KCl				
ENTH	$(2.9 \pm 0.5) \times 10^4$	$(9.7 \pm 0.8) \times 10^{-3}$	$(3.3 \pm 0.6) \times 10^{-7}$	14
ANTH	NM	NM	NM	

[a] Increase in K_d relative to binding POPC/POPE/PtdIns(4,5)P_2 (77:20:3) vesicles.
[b] Not measurable.

effect of PtdIns(4,5)P_2 on the membrane penetration of the ENTH domain. Increasing the ionic strength of medium (*i.e.* from 0.16 to 0.5 M KCl) slowed the adsorption of the ENTH domain to POPC/POPE/PtdIns(4,5)P_2 (77:20:3) vesicles by 45-fold (*i.e.* smaller k_a) but prolonged its membrane residence by 3-fold (*i.e.* smaller k_d). In contrast, the binding of the AP180 ANTH domain to the same vesicles was not detectable in the presence of 0.5 M KCl, again indicating that the ANTH domain interacts mainly with the membrane surface by nonspecific electrostatic interactions. Together, these results indicate that while the membrane association of both the epsin ENTH domain and the AP180 ANTH domain is driven primarily by nonspecific electrostatic interactions, the membrane dissociation of the former is uniquely governed by hydrophobic forces, due to its PtdIns(4,5)P_2-induced membrane penetration.

Mutational Analysis of the Epsin ENTH Domain—To investigate the membrane penetration mechanism of the ENTH domain, we mutated the hydrophobic Leu^6 and Met^{10} residues on helix 0 to glutamine and tested the effects on monolayer penetration. The L6Q and M10Q mutants bind the PtdIns(4,5)P_2 headgroup with nearly wild-type affinity, whereas liposome tubulation is abolished (8). As shown in Fig. 2, the L6Q and M10Q mutations greatly reduced the monolayer penetration of the epsin ENTH domain to the POPC/POPE/PtdIns(4,5)P_2 (77:20:3) monolayer, indicating the importance of the hydrophobic residues on helix 0 in PtdIns(4,5)P_2-induced membrane penetration. This reduction in penetration was PtdIns(4,5)P_2 specific, as these mutations did not greatly reduce the penetration into a POPC/POPE (80:20) monolayer (data not shown). In contrast, the mutation of Arg^{114} to Ala had little effect on the monolayer penetration. Finally, a double-site mutation of PtdIns(4,5)P_2-binding residues (R63L/H73L) caused significantly reduced penetration to the POPC/POPE/PtdIns(4,5)P_2 (77:20:3) monolayer, supporting the notion that PtdIns(4,5)P_2 binding is prerequisite for the membrane penetration of helix 0. The reason this mutation did not have as a dramatic effect as the L6Q and M10Q mutations was likely to be due to intrinsically high monolayer penetration power of R63L/H73L caused by the introduction of two hydrophobic residues near the membrane binding surface. This notion is supported by the finding that R63L/H73L could penetrate the POPC/POPE (80:20) monolayer almost as effectively as the POPC/POPE/PtdIns(4,5)P_2 (77:20:3) monolayer (see Fig. 2).

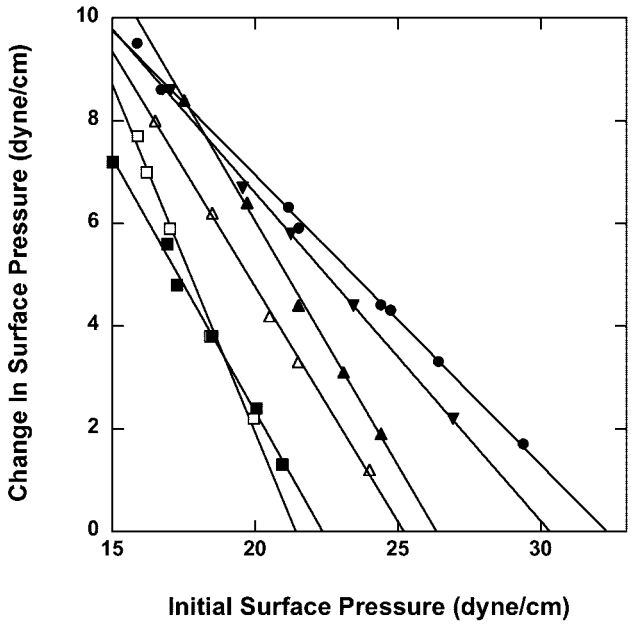

FIG. 2. **Effects of mutations on the monolayer penetration of epsin-ENTH.** Penetration of wild-type epsin ENTH (●), L6Q (□), M10Q (■), R63L/H73L (▲), and R114A (▼) into a POPC/POPE/PtdIns(4,5)P_2 (77:20:3) monolayer was monitored as a function of π_o. For R63L/H73L, the penetration was also measured with a POPC/POPE (80:20) monolayer (△). The subphase was 10 mM HEPES buffer, pH 7.4, with 0.16 M KCl for all measurements.

We then measured the vesicle binding of these mutants by the SPR analysis. For POPC/POPE/PtdIns(4,5)P_2 (77:20:3) vesicles, R63L/H73L showed extremely low affinity ($K_d > 25\ \mu M$), underscoring the importance of PtdIns(4,5)P_2 binding in the overall membrane affinity of the ENTH domain. It should be noted that although this mutant has the higher intrinsic monolayer penetrating ability (see above), it still cannot penetrate the PtdIns(4,5)P_2–containing vesicles (*i.e.* $\pi_c < 30$ dyne/cm) and has a drastically reduced positive electrostatic potential, which may be important for initial electrostatic vesicle binding (see below). L6Q and M10Q had 12- and 38-fold lower affinity, respectively, than the wild type, primarily due to larger k_d values. The faster membrane dissociation of these mutants is

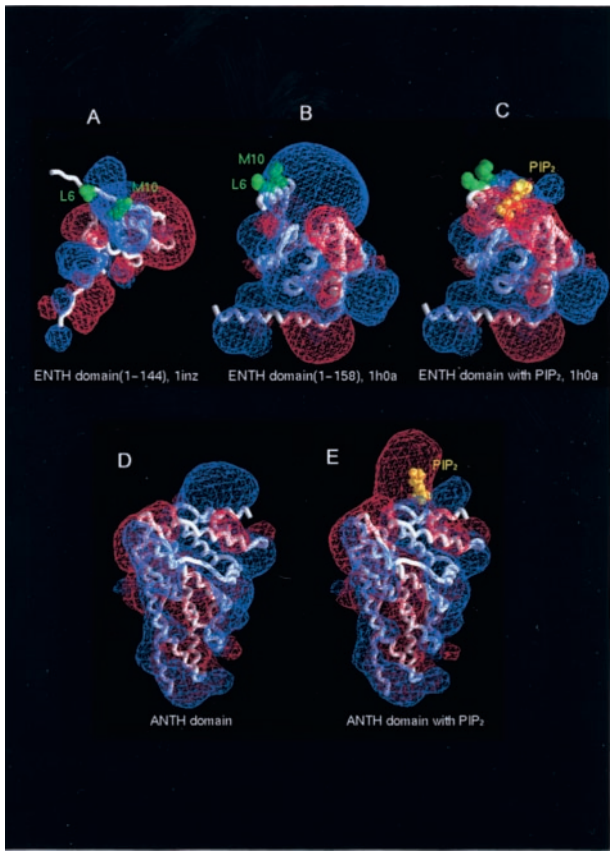

FIG. 3. **Effects of PtdIns(4,5)P_2 on the electrostatic potential of epsin ENTH and AP180-ANTH.** The electrostatic potentials for the ENTH and ANTH domain were calculated and visualized in the program GRASP by two-dimensional equipotentials contours in 0.1 M KCl. The *red* and *blue* contours represent −25 mV and +25 mV, respectively. *A*, ENTH (free structure) in the absence of Ins(1,4,5)P_3, *B*, ENTH (Ins(1,4,5)P_3-induced structure) in the absence of Ins(1,4,5)P_3, *C*, ENTH (Ins(1,4,5)P_3-induced structure) in the presence of Ins(1,4,5)P_3, *D*, ANTH in the absence of Ins(1,4,5)P_3, *E*, ANTH in the presence of Ins(1,4,5)P_3. The coordinates were taken from the structures of free epsin ENTH (1INZ) (32), Ins(1,4,5)P_3-bound epsin ENTH (1H0A) (8), and CALM ANTH (1HFA) (7).

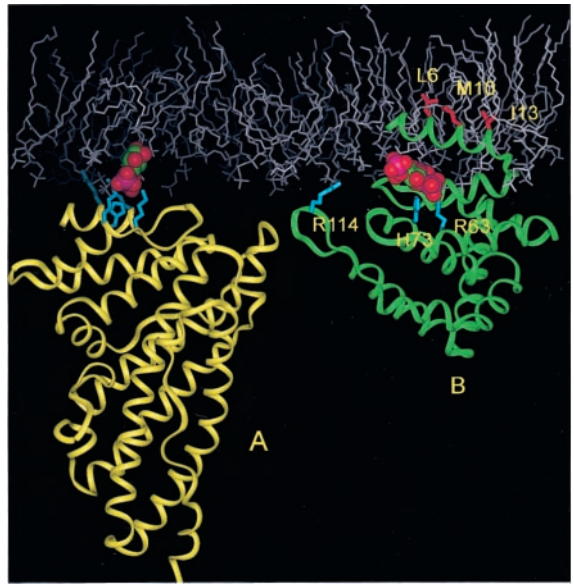

FIG. 4. **Proposed membrane binding mechanisms for the ENTH and ANTH domains.** The ANTH domain (*A*) binds to PtdIns(4,5)P_2-containing membranes primarily through electrostatic interactions with PtdIns(4,5)P_2 acting as a bridge. Only minor changes in protein conformation and membrane structure are expected. Ins(1,4,5)P_3 is shown in space filling representation and the side chains of PtdIns(4,5)P_2-binding basic residues are shown in *aqua*. For the epsin ENTH domain (*B*), nonspecific electrostatic interactions initially bring the protein to the membrane surface, which induces the formation of helix 0 and the PtdIns(4,5)P_2-binding pocket. The subsequent PtdIns(4,5)P_2 binding locks this conformation and concomitantly causes the hydrophobic residues in the helix to insert into the membrane. This membrane insertion elongates the membrane residence time of the protein and triggers the membrane deformation. Ins(1,4,5)P_3 is shown in space filling representation. The side chains of basic residues and hydrophobic residues are shown in *aqua* and *red*, respectively. The coordinates are taken from the x-ray structures of CALM ANTH (7) and epsin ENTH domain (8).

consistent with their less favorable hydrophobic interaction with the membrane. R114A had 4-fold lower K_d, due to a smaller k_a. Although this residue is not part of the PtdIns(4,5)P_2-binding site, it is on the same side of the putative membrane binding surface (see Fig. 4) and could contribute to nonspecific electrostatic interactions.

Calculation of Electrostatic Potential—To account for the differences in PtdIns(4,5)P_2-mediated membrane binding properties of the epsin ENTH domain and the AP180 ANTH domain, we calculated the electrostatic potential for these domains in the absence and presence of Ins(1,4,5)P_3 that is a soluble analog of PtdIns(4,5)P_2. It was shown that PtdIns(4,5)P_2 binding causes a local conformation change of the ENTH domain involving the formation of helix 0 (8). However, it is not known as to which conformation the epsin ENTH domain would assume when it initially contacts the PtdIns(4,5)P_2-containing membrane surface (*i.e.* a membrane-bound PtdIns(4,5)P_2-free conformation). Thus, the electrostatic potential of the ENTH domain in the absence of Ins(1,4,5)P_3 was calculated for the structures both before and after the conformational change. As shown in Fig. 3, *A* and *B*, strong positive potentials were seen near the PtdIns(4,5)P_2-binding pocket for both structures of Ins(1,4,5)P_3-free epsin ENTH, due to the presence of basic residues involved in PtdIns(4,5)P_2 binding (*i.e.* Arg^8, Lys^{11}, Arg^{25}, Arg^{63}, Lys^{69}, and His^{73}). These positive potentials may initially contribute to recruiting the domain to the anionic membrane surface through nonspecific electrostatic attraction, which subsequently leads to productive PtdIns(4,5)P_2 binding. Notice that the high positive potential of the induced structure (Fig. 3*B*) also surrounds the hydrophobic residues (*i.e.* Leu^6 and Met^{10}) of helix 0, which is expected to produce an energy barrier against the penetration of these residues into the low dielectric membrane interface. This is because the desolvation that is prerequisite for their membrane penetration would disrupt favorable interactions between water molecules and charged and polar groups on both the protein and the membrane. Interestingly, the positive potential of the epsin ENTH domain is dramatically reduced when PtdIns(4,5)P_2 binds to the domain (Fig. 3*C*). This suggests that PtdIns(4,5)P_2 may serve as an electrostatic switch to decrease the highly positive potential surrounding the hydrophobic residues on helix 0, thereby facilitating their membrane penetration. Thus, it would seem that for the ENTH domain PtdIns(4,5)P_2 plays a dual role of inducing a conformation change and switching the electrostatic potential.

Electrostatic potentials calculations of the ANTH domain are also consistent with our monolayer and SPR data. As shown in Fig. 3*D*, the ANTH domain has a lower positive electrostatic potential than the ENTH domain in the absence of PtdIns(4,5)P_2 (Fig. 3*B*), which is consistent with its smaller k_a. The docking of PtdIns(4,5)P_2 to the ANTH domain leads to a charge neutralization (Fig. 3*E*), but unlike the ENTH domain, the ANTH domain lacks hydrophobic residues on the membrane binding surface that would productively interact with the membrane. As a result, the electrostatic switch by

PtdIns(4,5)P_2 has no functional consequences for the ANTH domain. Taken together, our electrostatic calculations supported the notion that PtdIns(4,5)P_2 plays differential roles in the membrane binding of ENTH and ANTH domains.

DISCUSSION

Clathrin-mediated endocytosis involves a number of accessory proteins that control vesicle budding through protein-protein and lipid-protein interactions (40). Although it was long thought that clathrin is sufficient to drive membrane budding, recent evidence has established that the membrane bending requires concerted action of these accessory proteins (41). Among these proteins, epsin (8), dynamin (42), amphiphysin (43), and endophilin (44) have been shown to be able to cause liposome tubulation independently *in vitro*. However, questions remain as to whether all these proteins are directly involved in vesicle budding *in vivo* and how they initiate the vesicle budding. The present study provides some mechanistic insight into how epsin initiates the membrane curvature through lipid-protein interactions.

A recent study showed that the ENTH domain of epsin was as effective as the full-length protein in causing liposome tubulation, while neither AP180 nor its ANTH domain could induce the liposome tubulation independently (8). A main structural difference between the ENTH domain and the ANTH domain lies in the ligand-binding site (8). The ANTH domain does not have a well defined PtdIns(4,5)P_2-binding pocket and instead uses surface exposed basic residues to coordinate the ligand. The ENTH domain also lacks a well defined ligand-binding pocket; however, for this domain the formation of the pocket is triggered by PtdIns(4,5)P_2 binding. The same conformational change also aligns the hydrophobic residues, Leu^6, Met^{10}, and Ile^{13}, toward the membrane surface. These structural differences between the two domains are translated into their distinct membrane binding properties. Our monolayer measurements clearly show that the ENTH domain can penetrate the PtdIns(4,5)P_2-containing monolayer much more efficiently than the ANTH domain. Most significant, PtdIns(4,5)P_2 specifically triggers the penetration of the ENTH domain, but not the ANTH domain, into the monolayer whose surface packing density recapitulates those of cell membranes and large unilamellar vesicles. Neither other phosphoinositides nor phosphatidylserine can replace the effect of PtdIns(4,5)P_2 on the ENTH domain. This is similar to specific membrane penetration of FYVE domains and the PX domain of $p40^{phox}$ induced by phosphatidylinositol 3-phosphate (26, 33). Monolayer penetration properties of the ENTH domain mutants also verify the notion that hydrophobic residues on the same face of induced helix 0 are responsible for the membrane penetration of the ENTH domain.

Our SPR measurements and electrostatic potential calculations provide further insight into the differential PtdIns(4,5)P_2dependent membrane binding mechanisms of these two domains. The epsin ENTH domain binds the same PtdIns(4,5)P_2-containing vesicles with 12-fold greater affinity than the AP180 ANTH domain, due to faster association and slower dissociation. The faster membrane association of the epsin ENTH domain can be accounted for by its more positive electrostatic potential on its putative membrane binding surface, due to basic residues in the PtdIns(4,5)P_2-binding pocket and Arg^{114} (see Fig. 3). The slower dissociation of epsin ENTH is consistent with the higher degree of monolayer penetration by its hydrophobic residues, including Leu^6 and Met^{10}. The 12- and 38-fold reductions in affinity by L6Q and M10Q mutations, respectively, indicate that membrane penetration of these residues contributes significantly to overall membrane binding of the ENTH domain.

Variation of the PtdIns(4,5)P_2 concentration and the ionic strength of the medium also underscores the different roles PtdIns(4,5)P_2 play in membrane binding of the two domains. In the case of the ENTH domain, PtdIns(4,5)P_2 enhances k_a via electrostatic protein-PtdIns(4,5)P_2 interactions, whereas it lowers k_d by inducing membrane penetration of the hydrophobic residues, and thereby allowing hydrophobic interactions. For the ANTH domain, on the other hand, PtdIns(4,5)P_2 would seem to simply function as a bridge between the domain and the membrane, as suggested for the role of calcium in the membrane binding of annexins (45). This is due to the presence of pre-aligned basic residues and the absence of hydrophobic residues on the PtdIns(4,5)P_2 binding surface.

Based on these data, we propose differential membrane binding mechanisms for the two domains (see Fig. 4). The epsin ENTH domain initially binds to PtdIns(4,5)P_2-containing anionic membranes by nonspecific electrostatic interactions. The nature of membrane-bound PtdIns(4,5)P_2-free conformation is not known at present. However, it would be reasonable to assume that the initial membrane contact induces, at least partially, the formation of the helix 0 and hence the PtdIns(4,5)P_2-binding pocket, since the induction of amphipathic helices at the water-membrane interface has been well documented (46–48). The subsequent PtdIns(4,5)P_2 binding would then lock this induced conformation, as shown in the crystal structure of the epsin ENTH-Ins(1,4,5)P_3 complex (8), concomitantly inducing the hydrophobic residues in the helix to insert into the membrane by the electrostatic switch mechanism. This membrane insertion elongates the membrane residence time of the protein and triggers the membrane deformation. For the ANTH domain, membrane-protein binding takes place primarily through electrostatic interactions with PtdIns(4,5)P_2 acting as a bridge. Only minor changes in protein conformation and membrane structure are expected.

Multiple steps of complex protein-protein and protein-lipid interactions are involved in the vesicle budding. Our results strongly suggest that the PtdIns(4,5)P_2-triggered membrane penetration of the ENTH domain is a critical step in the epsin-induced membrane curvature. This notion is supported by much reduced monolayer penetration of L6Q and M10Q mutants that have lost the liposome tubulation activity of the wild type epsin ENTH domain. The penetration of the ENTH domain into the PtdIns(4,5)P_2-rich region of the plasma membrane would cause the positive membrane curvature, which has been suggested to be essential for membrane budding (49). Intriguingly, there are many peripheral proteins, including phosphoinositide-specific FYVE domains and PX domains, which penetrate lipid monolayers as well as or more effectively than the epsin ENTH domain without inducing liposome tubulation. Perhaps the insertion of a relatively rigid α-helix distorts the membrane enough to cause curvature, while insertion of a less ordered loop may be insufficient. Further mechanistic studies on the membrane-ENTH domain interactions would reveal the molecular basis of this special activity of the epsin ENTH domain.

REFERENCES

1. Marsh, M., and McMahon, H. T. (1999) *Science* **285,** 215–220
2. Schmid, S. L. (1997) *Annu. Rev. Biochem.* **66,** 511–548
3. Brodsky, F. M., Chen, C. Y., Knuehl, C., Towler, M. C., and Wakeham, D. E. (2001) *Annu. Rev. Cell Dev. Biol.* **17,** 517–568
4. Hinshaw, J. E. (2000) *Annu. Rev. Cell Dev. Biol.* **16,** 483–519
5. Cremona, O., and De Camilli, P. (2001) *J. Cell Sci.* **114,** 1041–1052
6. Itoh, T., Koshiba, S., Kigawa, T., Kikuchi, A., Yokoyama, S., and Takenawa, T. (2001) *Science* **291,** 1047–1051
7. Ford, M. G., Pearse, B. M., Higgins, M. K., Vallis, Y., Owen, D. J., Gibson, A., Hopkins, C. R., Evans, P. R., and McMahon, H. T. (2001) *Science* **291,** 1051–1055
8. Ford, M. G., Mills, I. G., Peter, B. J., Vallis, Y., Praefcke, G. J., Evans, P. R., and McMahon, H. T. (2002) *Nature* **419,** 361–366
9. Itoh, T., and Takenawa, T. (2002) *Cell Signal.* **14,** 733–743

10. Hurley, J. H., and Wendland, B. (2002) *Cell* **111,** 143–146
11. Nossal, R., and Zimmerberg, J. (2002) *Curr. Biol.* **12,** R770–R772
12. Kay, B. K., Yamabhai, M., Wendland, B., and Emr, S. D. (1999) *Protein Sci.* **8,** 435–438
13. De Camilli, P., Chen, H., Hyman, J., Panepucci, E., Bateman, A., and Brunger, A. T. (2002) *FEBS Lett.* **513,** 11–18
14. Lohi, O., Poussu, A., Mao, Y., Quiocho, F., and Lehto, V. P. (2002) *FEBS Lett.* **513,** 19–23
15. Kates, M. (1986) *Techniques of Lipidology*, 2nd Ed., pp. 114–115, Elsevier Science Publishers B. V., Amsterdam
16. Ho, S. N., Hunt, H. D., Horton, R. M., Pullen, J. K., and Pease, L. R. (1989) *Gene* (*Amst.*) **77,** 51–59
17. Bittova, L., Sumandea, M., and Cho, W. (1999) *J. Biol. Chem.* **274,** 9665–9672
18. Nalefski, E. A., and Falke, J. J. (1998) *Biochemistry* **37,** 17642–17650
19. Ball, A., Nielsen, R., Gelb, M. H., and Robinson, B. H. (1999) *Proc. Natl. Acad. Sci. U. S. A.* **96,** 6637–6642
20. Frazier, A. A., Wisner, M. A., Malmberg, N. J., Victor, K. G., Fanucci, G. E., Nalefski, E. A., Falke, J. J., and Cafiso, D. S. (2002) *Biochemistry* **41,** 6282–6292
21. Verger, R., and Pattus, F. (1982) *Chem. Phys. Lipids* **30,** 189–227
22. Cho, W., Bittova, L., and Stahelin, R. V. (2001) *Anal. Biochem.* **296,** 153–161
23. Bittova, L., Stahelin, R. V., and Cho, W. (2001) *J. Biol. Chem.* **276,** 4218–4226
24. Stahelin, R. V., and Cho, W. (2001) *Biochemistry* **40,** 4672–4678
25. Stahelin, R. V., and Cho, W. (2001) *Biochem. J.* **359,** 679–685
26. Stahelin, R. V., Long, F., Diraviyam, K., Bruzik, K. S., Murray, D., and Cho, W. (2002) *J. Biol. Chem.* **277,** 26379–26388
27. Myszka, D. G. (1997) *Curr. Opin. Biotechnol.* **8,** 50–57
28. Schuck, P. (1997) *Annu. Rev. Biophys. Biomol. Struct.* **26,** 541–566
29. Nicholls, A., Sharp, K. A., and Honig, B. (1991) *Proteins* **11,** 281–296
30. Honig, B., and Nicholls, A. (1995) *Science* **268,** 1144–1149
31. Brooks, B., Bruccoleri, R., Olafson, B., States, D., Swaminathan, S., and Karplus, M. (1983) *J. Comp. Chem.* **4,** 187–217
32. Koshiba, S., Kigawa, T., Kikuchi, A., and Yokoyama, S. (2001) *J. Struct. Funct. Genom.* **2,** 1–8
33. Stahelin, R. V., Burian, A., Bruzik, K. S., Murray, D., and Cho, W. (2003) *J. Biol. Chem.* **278,** 14469–14479
34. Lichtenbergova, L., Yoon, E. T., and Cho, W. (1998) *Biochemistry* **37,** 14128–14136
35. Medkova, M., and Cho, W. (1998) *Biochemistry* **37,** 4892–4900
36. Medkova, M., and Cho, W. (1998) *J. Biol. Chem.* **273,** 17544–17552
37. Blume, A. (1979) *Biochim. Biophys. Acta* **557,** 32–44
38. Demel, R. A., Geurts van Kessel, W. S., Zwaal, R. F., Roelofsen, B., and van Deenen, L. L. (1975) *Biochim. Biophys. Acta* **406,** 97–107
39. Marsh, D. (1996) *Biochim. Biophys. Acta* **1286,** 183–223
40. Higgins, M. K., and McMahon, H. T. (2002) *Trends Biochem. Sci.* **27,** 257–263
41. Nossal, R. (2001) *Traffic* **2,** 138–147
42. Sweitzer, S. M., and Hinshaw, J. E. (1998) *Cell* **93,** 1021–1029
43. Takei, K., Slepnev, V. I., Haucke, V., and De Camilli, P. (1999) *Nat. Cell Biol.* **1,** 33–39
44. Farsad, K., Ringstad, N., Takei, K., Floyd, S. R., Rose, K., and De Camilli, P. (2001) *J. Cell Biol.* **155,** 193–200
45. Swairjo, M. A., Concha, N. O., Kaetzel, M. A., Dedman, J. R., and Seaton, B. A. (1995) *Nat. Struct. Biol.* **2,** 968–974
46. Anantharamaiah, G. M., Jones, J. L., Brouillette, C. G., Schmidt, C. F., Chung, B. H., Hughes, T. A., Bhown, A. S., and Segrest, J. P. (1985) *J. Biol. Chem.* **260,** 10248–10255
47. Wald, J. H., Krul, E. S., and Jonas, A. (1990) *J. Biol. Chem.* **265,** 20037–20043
48. Keller, R. C., Killian, J. A., and de Kruijff, B. (1992) *Biochemistry* **31,** 1672–1677
49. Huttner, W. B., and Schmidt, A. A. (2002) *Trends Cell Biol.* **12,** 155–158